Lawrence Berkeley National Laboratory
Lawrence Berkeley National Laboratory

Title
Mask roughness challenges in extreme ultraviolet mask development

Permalink
https://escholarship.org/uc/item/095087tg

Author
Naulleau, Patrick

Publication Date
2011-10-28

eScholarship.org Powered by the California Digital Library
University of California

Mask roughness challenges in extreme ultraviolet mask development

Patrick Naulleau,[1] Brittany McClinton,[2] Kenneth A. Goldberg,[1]
Iacopo Mochi,[1] and Abbas Rastegar[3]

[1] Center for X-Ray Optics, Lawrence Berkeley National Laboratory, Berkeley, CA 94720
[2] Applied Sci. & Technol. Graduate Group, University of California, Berkeley, CA 94720
[3] SEMATECH, Albany, NY 12203

Abstract

Despite significant progress in the commercialization of extreme ultraviolet (EUV) lithography, many challenges remain. Although availability of a reliable high power source is arguably the most daunting of these challenges, important mask issues are also of major concern. The issues of EUV phase roughness that can arise from either multilayer or capping layer roughness has recently become of increasing concern. The problem with mask phase roughness is that it couples to image plane speckle and thus line-edge roughness (LER). The coupling, however, depends on many factors including roughness magnitude, roughness correlation length, illumination partial coherence, aberrations and defocus, and numerical aperture. Analysis shows that only on the order of 50 pm multilayer roughness may be tolerable at the 22-nm half-pitch node. The analysis, however, also shows that the difficulty does not scale with future node reductions. Moreover, it is found that ruthenium is a particularly bad choice for capping layer from the perspective of phase roughness and that cleaning damage in such a multilayer could lead to unacceptable image-plane LER.

1. Introduction

Despite significant progress in the commercialization of extreme ultraviolet (EUV) lithography [1], important challenges remain. Although availability of a reliable high power source [2-4] is arguably the most daunting of these challenges, several mask issues are also of major concern. The most pressing and well known of these issues is mask defectivity [5]. Significant progress has been made in this area, but another two orders of magnitude defect reduction is still required to meet current pilot lines goals [5]. As described in the literature [6], as a work around to the availability of zero defect mask blanks, a variety of methods have been proposed including defect repair, defect

compensation, and defect hiding with pattern shift. Another significant concern for EUV masks is critical dimension uniformity (CDU) and in particular effective CDU at the wafer. The non-telecentric nature of EUV masks due to the requisite off-axis illumination, raises a variety of EUV specific problems. A thorough survey of the various sources of mask-induced CDU has been presented by Gallagher *et al.* [7].

Another important EUV mask concern [8-11] is phase roughness that can arise from either multilayer or capping layer roughness and lead the image plane speckle and in turn line-edge roughness (LER). The visibility of, and concern over, this problem has recently increased since its experimental demonstration at EUV [12] in both an microfield exposure tool [13] and a full field EUV alpha tool [7]. The coupling from roughness to LER, however, depends on many factors including roughness magnitude, roughness correlation length, illumination partial coherence, aberrations and defocus, and numerical aperture (NA). Here we study these various factors in detail presenting sensitivity trends and providing guidance for system design choices of the future.

2. Modeling methodology

The simplified model we use to derive all the results in the following sections relies on scalar aerial image computation software based on the partially-coherent image formation equations [14]. Similar capabilities can also be obtained through the use of commercial modeling packages such as Prolith [15] and HyperLith [16]. In this model, the multilayer roughness is modeled as in-plane phase variations in the object plane. Accounting for reflection from the Bragg structure and assuming the structure to be intact throughout at least the top 10 layers of the multilayer stack, the phase variations are set to two times the multilayer height variations to be modeled. A detailed description of this modeling technique can be found in Ref. [10]. We note that the validity of the two-dimensional modeling used here as a simplification of an inherently three-dimensional structure has been verified [17]. It is also crucial to understand that the roughness of concern is that roughness which it replicated through at least to top 10 layers of the Molybdenum/Silicon reflector stack [17]. We refer to this roughness as replicated surface roughness (RSR).

3. Coupling from roughness to LER

As stipulated above, mask phase roughness couples to LER through the generation of image-plane speckle, or random intensity variations. The reason that a pure phase

distribution translates to intensity variations at the wafer is that the imaging system itself is band-limited meaning that even an aberration-free system cannot faithfully reproduce the exact electric field and failure to do so means that the magnitude squared of the electric field can no longer be perfectly uniform. The problem becomes even more severe as we deviate from an ideal system by, for example, moving out of focus. Moving out of focus is identical to observing the electric field after propagation a certain distance away from the mask. This process causes points with random phase to mix and interfere causing speckle [5]. Another way to view this process is through a concept known as transport of intensity [18-20] where random wavefront curvatures in one plane causes ray bundle concentration (intensity) variations in another plane.

From the discussion above, it is evident that coherence would be expected to play an important role in the generation of LER. Thus, we begin this study by explicitly considering illumination partial coherence (Fig. 1). In these results, we assume a half pitch of 22 nm, a NA of 0.32, on-axis disk illumination, flare of 5%, RSR of 100-pm, roughness correlation length of 100 nm, and a roughness exponent of 1. The graph in Fig. 1 shows the resulting image plane line-width roughness (LWR) as a function of partial coherence (Sigma) for various amounts of defocus. The maximum defocus considered is $0.5\lambda/NA^2$. At the edge of focus we see the unsurprising results of nearly linear dependence on Sigma, with the LWR increasing as the Sigma is decreased. Also as one might expect, the dependence on Sigma is much weaker as we move closer to focus. More surprising, however, is the strongly non-linear behavior when out of focus, but not at the edge of focus. At a defocus value of $0.33\lambda/NA^2$, we see little negative impact of dropping Sigma below 0.5. This fact could have significant implications for the future viability resolution enhancing modified illumination. We note that the nonlinearity can be shown to depend on the ratio of the roughness correlation length to the NA.

Certainly the LWR is expected to be dependent on the RSR magnitude. Understanding this dependence is crucial to developing mask specifications. Figure 2 shows the results for a 0.32 NA system imaging 22-nm half-pitch lines. Also assumed is disk illumination with a Sigma of 0.5, flare of 5%, roughness correlation length of 100 nm, and roughness exponent of 1. In this case we find linear dependence on RSR with

increasing slope as a function of defocus. The slope at defocus levels of 0 nm, 25 nm, 50 nm, and 75 nm, is 1.0×10^{-6}, 5.0×10^{-6}, 1.18×10^{-5}, and 2.53×10^{-5}, respectively.

As suggested by our specification of the roughness correlation length and roughness exponent, defining surface roughness as a single magnitude is incomplete. Next we explicitly consider the impact of roughness correlation length on the LWR (Fig. 3). In this case, we again assume 0.32 NA, 22-nm half-pitch lines, disk illumination with a Sigma of 0.5, flare of 5%, RSR of 100 pm, and roughness exponent of 1. These results show a peaked behavior with the peak occurring approximately at 1.4λ/NA. For the 0.32-NA system in Fig. 3, this corresponds to a correlation length of 60 nm. The nearly factor of 3 change in LWR seen as a function of correlation length for the same roughness magnitude demonstrates the importance of specifying the higher order statistics of the mask roughness.

We note that the peak position seen in Fig. 3 is relatively close to the experimentally measured RSR correlation length of 100 nm for a magnetron coating process. Most EUV mask blanks, however, are actually fabricated using ion-beam deposition, thus it would be important to characterize the RSR correlation length for this process as well yet we do not expect it to be significantly different. Also, given the desire to smooth out defects using the multilayer process, it is unrealistic to expect the correlation length of future masks to be pushed towards the short end of the plot in Fig. 3 where the LWR is seen to quickly reduce.

The third metric required to fully describe a fractal self-affine surface is the roughness exponent. Figure 4 shows the LWR results assuming 0.32 NA, 22-nm half-pitch lines, disk illumination with a Sigma of 0.5, flare of 5%, RSR of 100 pm, and correlation length of 100 nm. In this case the response is seen to be linear with the roughness exponent (α) which simply modulates the amount of roughness in the passband of interest. Thus the roughness exponent has a similar effect as directly changing the RSR.

Finally we consider the effect of changing the NA (Fig. 5). At the same time, however, we also proportionally change the CD and the defocus range, thus explicitly considering future technology nodes. In all cases the Sigma is kept at 0.5, flare kept at 5%, roughness correlation length kept at 100 nm, RSR kept at 100 pm, and roughness

exponent kept at 1. The plot shows the counterintuitive behavior of decreasing sensitivity to roughness as we look to future generations, suggesting that the RSR problem gets easier in the future. This occurs because increasing the NA causes the correlation length peak (as seen in Fig. 3) to move to shorter values whereas the actual mask correlation length remains fixed. This thus causes the resulting LWR to decrease.

In order to assess the difficulty as a function of NA, we also need to account for the fact that the LWR requirements scale down as a function of technology node. The plot in Fig. 6 addresses this by normalizing the LWR by the CD and the LWR at 0.32 NA for each focus level. A value of 1 represents the difficultly at 0.32 NA and is inversely proportional to the required RSR to meet the LWR requirements. Decreasing values represents less difficulty. As suggested by Fig. 5, we come to the counterintuitive conclusion that the difficulty indeed decreases with future technology nodes.

4. Effect of multilayer capping layer roughness

Much of the analysis in Section 3 implicitly assumed the phase roughness to be a result of RSR. Although RSR is the physical roughness source which mostly strongly couples to phase roughness, other sources of roughness can also be important, for example multilayer capping layer roughness. Unlike for the RSR, capping layer roughness couples to phase roughness by way of refraction, thus the optical properties of the capping layer must be taken into account. The most common capping layer for EUV mask multilayer stacks is ruthenium which provides a double-pass phase shift of 6° per nm of thickness [21]. Additionally, 1 nm of ruthenium attenuates the light by 3% in double pass. By contrast, silicon would provide only 0.0036° phase shift per nm of material double pass and 0.3% attenuation [21]. From this perspective, ruthenium does not appear to be an optimal choice for capping layer. Nevertheless, as-deposited ruthenium capping layers are more than adequately smooth for this not to be an issue.

The concern with the ruthenium capping layer arises when the mask is cleaned and the capping layer is potentially roughened. Figure 7 shows measured ruthenium capping layer roughness as a function of cleaning cycles using a conventional wet cleaning process [22]. Also shown is a linear fit to the data extrapolating the damage out to 30 cleaning cycles. This roughness data can then be used to predict the resulting LWR, but as discussed above we must also account for the roughness correlation length and

roughness exponent. Figure 8 shows the measured power spectrum for the roughness data in Fig. 7. From the power spectrum we extract a roughness correlation length of 15 nm and roughness exponent of 0.65. Finally, Fig. 9 shows the computed LWR for the measured and extrapolated ruthenium capping layer roughness. The results show near 1 nm LWR at the edge of focus after 30 cleaning cycles. The asymmetric through focus behavior is a result of combined phase and amplitude roughness in the reflected field.

We also note that the correlation length in this case is at the high slope region as seen in Fig. 3. This suggests that the results shown in Fig. 9 will be quite sensitive to the morphology of the roughening that place during the cleaning process.

5. Summary

Mask roughness is a potentially significant source of image plane LWR in EUV lithography. The sensitivity of the induced LWR to roughness depends on many factors including illumination partial coherence, defocus, roughness correlation length, roughness exponent, and NA. The effect of partial coherence is to depend on focus in a complicated way with nonlinear behavior at focus values between the extremes of zero defocus and $0.5\lambda/NA^2$. Another interesting result is the strong dependence of LWR on the roughness correlation length. The nearly factor of 3 change in LWR demonstrates the importance of specifying the higher order statistics of the mask roughness. Also, under the assumption that the roughness correlation length will not scale down with future nodes, it was been shown that unlike most problems in lithography, the mask roughness induced LWR becomes less problematic at future nodes. We note, however that this is only true for RSR-induced LWR since in that case the correlation length lies on the long side of the peak. For capping-layer-roughness-induced LWR, we would not expect the same behavior because the correlation length lies on the short side of the peak. Thus as the NA is increased and the peak is moved to shorter correlation lengths, the coupling from roughness to LWR will increase. Thus the mask cleaning requirements from the damage perspective would be expected to become more challenging in the future.

6. Acknowledgements

The authors acknowledge the programmatic support from Dominic Ashworth, Bryan Rice, and Stefan Wurm of SEMATECH. This work was supported by SEMATECH and

the Director, Office of Science, of the U.S. Department of Energy under Contract No. DE-AC02-05CH11231..

References

1. C. Wagner, et al., “EUV lithography at chipmakers has started: performance validation of ASML's NXE:3100,” Proc. SPIE **7969**, 79691F (2011).

2. D. Brandt, et al. “LPP source system development for HVM,” Proc. SPIE **7969**, 79691H (2011).

3. Hakaru Mizoguchi, Hidenobu Kameda, Hiroaki Nakarai, and Junichi Fujimoto, “100W 1st generation laser-produced plasma light source system for HVM EUV lithography,” Proc. SPIE **7969**, 796908 (2011).

4. Masaki Yoshioka, Jeroen Jonkers, Max C. Schürmann, Rolf Apetz, Volker Kilian, and Marc Corthout, “Tin DPP source collector module (SoCoMo) ready for integration into Beta scanner,” Proc. SPIE **7969**, 79691G (2011).

5. F. Goodwin, T. Nakajima, P. Kearney, J. Kageyama, V. Jindal, M. Kishimoto, C. Lin, A. Ma, M. Godwin, and J. Harris-Jones, “SEMATECH's EUVL Mask Blank Defect Reduction Program: ML Deposition Defect Sources and Mitigation Strategies,” 2010 International Symposium on Extreme Ultraviolet Lithography, Kobe, Japan, October 18-20, 2010, proceedings available from SEMATECH, Austin, TX.

6. T. Liang, G. Zhang, S. Son, R. Chen, S. Lee, M. Leeson, P. Yan, A. Ma, L. He, G. Vandentop, “Strategy and Feasibility of Defect-free Mask Fabrication to Enable EUVL,” 2009 International Symposium on Extreme Ultraviolet Lithography, Prague, Czech Republic, October 18- October 23, 2009, proceedings available from SEMATECH, Austin, TX.

7. E. Gallagher, G. McIntyre, S. Raghunathan, L. Kindt, J. Whang, M. Barrett, T. Wallow, and O. Wood, “EUV masks under exposure: practical considerations,” Proc. SPIE **7969**, 79690W (2011).

8. N. Beaudry, T. Milster, “Effects of mask roughness and condenser scattering in EUVL systems,” Proc. SPIE. **3676**, 653-662 (1999).

9. P. Naulleau, “The relevance of mask-roughness-induced printed line-edge roughness in recent and future EUV lithography tests,” Appl. Opt. **43**, 4025-4032 (2004).

10. P. Naulleau, D. Niakoula, G. Zhang, "System-level line-edge roughness limits in extreme ultraviolet lithography," J. Vac. Sci. & Technol. B **26**, 1289-1293 (2008).
11. P. Naulleau and S. George, "Implications of image plane line-edge roughness requirements on extreme ultraviolet mask specifications," Proc. SPIE **7379**, 73790O-73790O-11 (2009).
12. P. Naulleau, "Correlation method for the measure of mask-induced line-edge roughness in extreme ultraviolet lithography," Appl. Opt. **48**, 3302-3307 (2009).
13. P. Naulleau, C. Anderson, P. Denham, S. George, K. Goldberg, B. Hoef, C. Koh, B. La Fontaine, W. Montgomery, J. Roller, T. Wallow, S. Wurm, "The SEMATECH Berkeley microfield exposure tool: learning at the 22-nm node and beyond," Proc. SPIE **7271**, 7271W (2009).
14. J. W. Goodman, *Statistical Optics*, John Wiley and Sons, New York, 1985, **Chap. 7**, 286-360.
15. Prolith is a registered trademark of KLA-Tencor Corporation, 160 Rio Robles, San Jose, California 95134.
16. EM-Suite is a registered trademark of Panoramic Technologies, www.panoramictech.com.
17. P. Naulleau and S. George, "Validity of the thin mask approximation in extreme ultraviolet mask roughness simulations," Appl. Opt., *to be published* (2011).
18. M. Teague, "Irradiance moments: their propagation and use for unique retrieval of phases," J. Opt. Soc. Am. **72**, 1199–1209 (1982).
19. N. Striebl, "Phase imaging by the transport of intensity equation," Opt. Commun. **49**, 6–10 (1984).
20. K. Ichikawa, A. Lohmann, and M. Takeda, "Phase retrieval based on the irradiance transport equation and the Fourier transport method," Appl. Opt. **27**, 3433–3436 (1988).
21. CXRO X-ray Materials Database (http://henke.lbl.gov/optical_constants/)
22. A. Rastegar, S. Eichenlaub, A. John, B. Lee, M. House, S. Huh, B. Cha, H. Yun, I. Mochi, and K. Goldberg, "Particle removal challenges with EUV patterned masks for the sub-22 nm HP node," Proc. SPIE 7636, 76360N (2010)
.

List of Figures

Fig. 1. Effect of partial coherence on image plane LWR. Assumptions include: Half pitch = 22 nm, NA = 0.32, on-axis disk illumination, flare = 5%, RSR = 100-pm, roughness correlation length = 100 nm, and roughness exponent = 1. Graph shows the resulting image plane line-width roughness (LWR) as a function of partial coherence (Sigma) for various amounts of defocus. The maximum defocus considered is $0.5\lambda/NA^2$.

Fig. 2. Dependence of LWR on RSR for a 0.32 NA system imaging 22-nm half-pitch lines. Also assumed is disk illumination with a Sigma of 0.5, flare of 5%, roughness correlation length of 100 nm, and roughness exponent of 1. Results show linear dependence on RSR with increasing slope as a function of defocus. The slope at defocus levels of 0 nm, 25 nm, 50 nm, and 75 nm, is 1.0×10^{-6}, 5.0×10^{-6}, 1.18×10^{-5}, and 2.53×10^{-5}, respectively.

Fig. 3. Impact of roughness correlation length on the LWR assuming 0.32 NA, 22-nm half-pitch lines, disk illumination with a Sigma of 0.5, flare of 5%, RSR of 100 pm, and roughness exponent of 1. Results show a peaked behavior with the peak occurring approximately at $1.4\lambda/NA$. For the 0.32-NA system considered here, this corresponds to a correlation length of 60 nm.

Fig. 4. LWR as a function of roughness exponent (α) assuming 0.32 NA, 22-nm half-pitch lines, disk illumination with a Sigma of 0.5, flare of 5%, RSR of 100 pm, and correlation length of 100 nm. Response is linear with the roughness exponent which serves to modulate the amount of roughness in the passband of interest. Thus the roughness exponent has a similar effect as directly changing the RSR.

Fig. 5. Effect of changing the NA with fixed k_1. Defocus range is scaled by NA^2, thus plot can be viewed as a function of half-pitch technology node shown as labels in the pole. In all cases the Sigma is kept at 0.5, flare kept at 5%, roughness correlation length kept at 100 nm, RSR kept at 100 pm, and roughness exponent kept at 1.

Fig. 6. Difficulty ($LWR/LWR_{0.32NA}/CD$) as a function of NA. A value of 1 represents the difficultly at 0.32 NA. Decreasing values represents less difficulty. Difficulty is inversely proportional to the required RSR to meet the LWR requirements.

Fig. 7. Measured ruthenium capping layer roughness as a function of cleaning cycles. Also shown is a linear fit to the data extrapolating the damage out to 30 cleaning cycles.

Fig. 8. Measured power spectrum for roughness data in Fig. 7.

Fig. 9. Computed LWR for the measured and extrapolated ruthenium capping layer roughness. The results show near 1 nm LWR at the edge of focus after 30 cleaning cycles. The asymmetric through focus behavior is a result of combined phase and amplitude roughness in the reflected field.

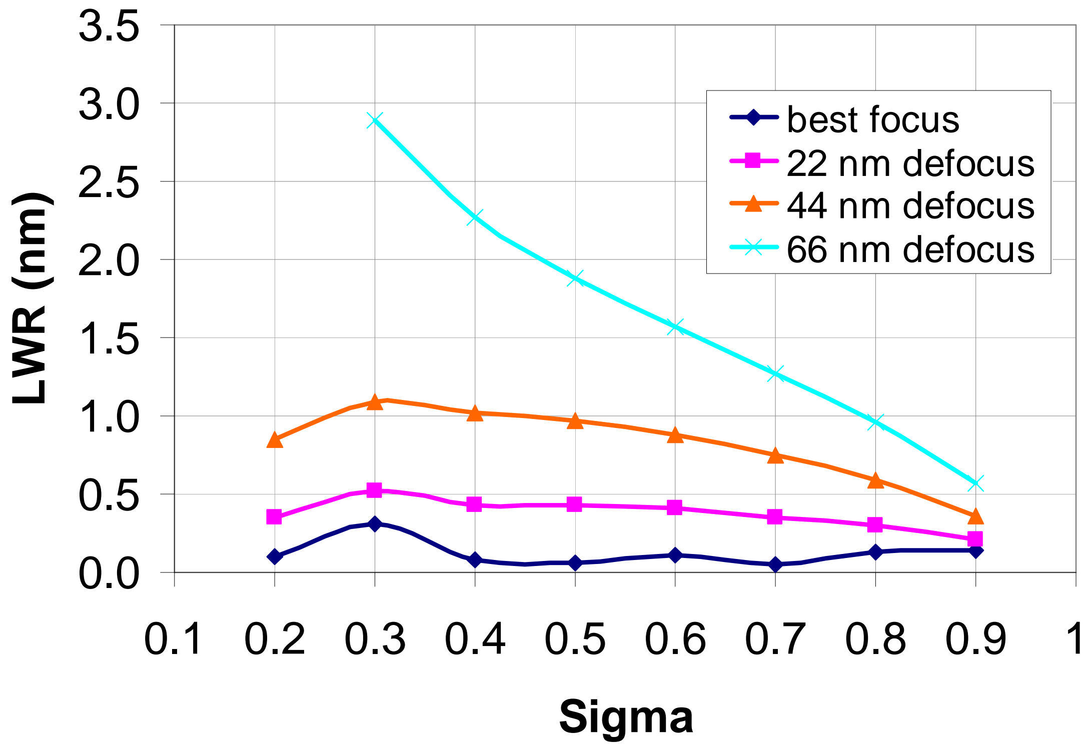

Fig. 1. Effect of partial coherence on image plane LWR. Assumptions include: Half pitch = 22 nm, NA = 0.32, on-axis disk illumination, flare = 5%, RSR = 100-pm, roughness correlation length = 100 nm, and roughness exponent = 1. Graph shows the resulting image plane line-width roughness (LWR) as a function of partial coherence (Sigma) for various amounts of defocus. The maximum defocus considered is $0.5\lambda/NA^2$.

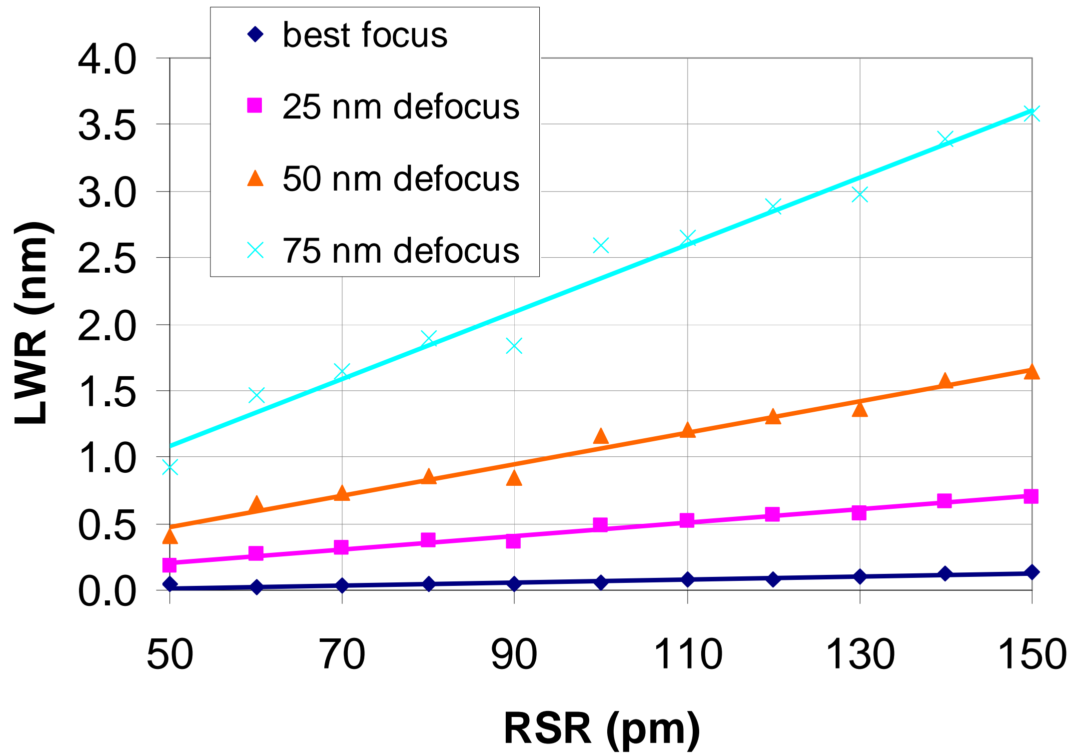

Fig. 2. Dependence of LWR on RSR for a 0.32 NA system imaging 22-nm half-pitch lines. Also assumed is disk illumination with a Sigma of 0.5, flare of 5%, roughness correlation length of 100 nm, and roughness exponent of 1. Results show linear dependence on RSR with increasing slope as a function of defocus. The slope at defocus levels of 0 nm, 25 nm, 50 nm, and 75 nm, is 1.0×10^{-6}, 5.0×10^{-6}, 1.18×10^{-5}, and 2.53×10^{-5}, respectively.

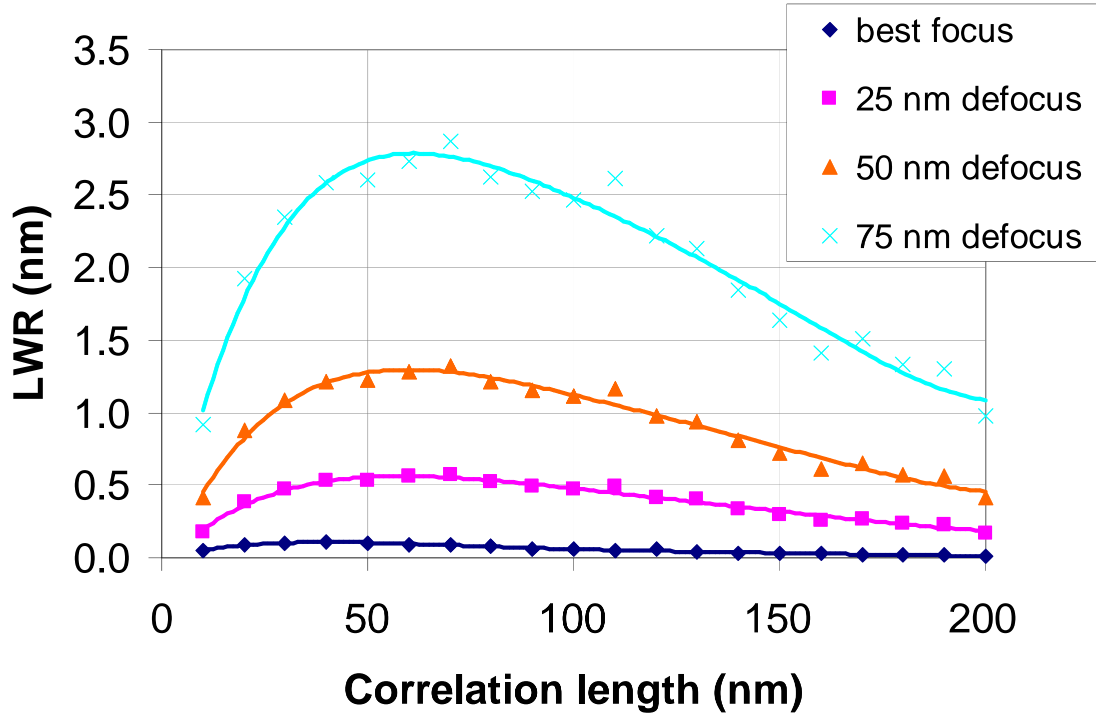

Fig. 3. Impact of roughness correlation length on the LWR assuming 0.32 NA, 22-nm half-pitch lines, disk illumination with a Sigma of 0.5, flare of 5%, RSR of 100 pm, and roughness exponent of 1. Results show a peaked behavior with the peak occurring approximately at 1.4λ/NA. For the 0.32-NA system considered here, this corresponds to a correlation length of 60 nm.

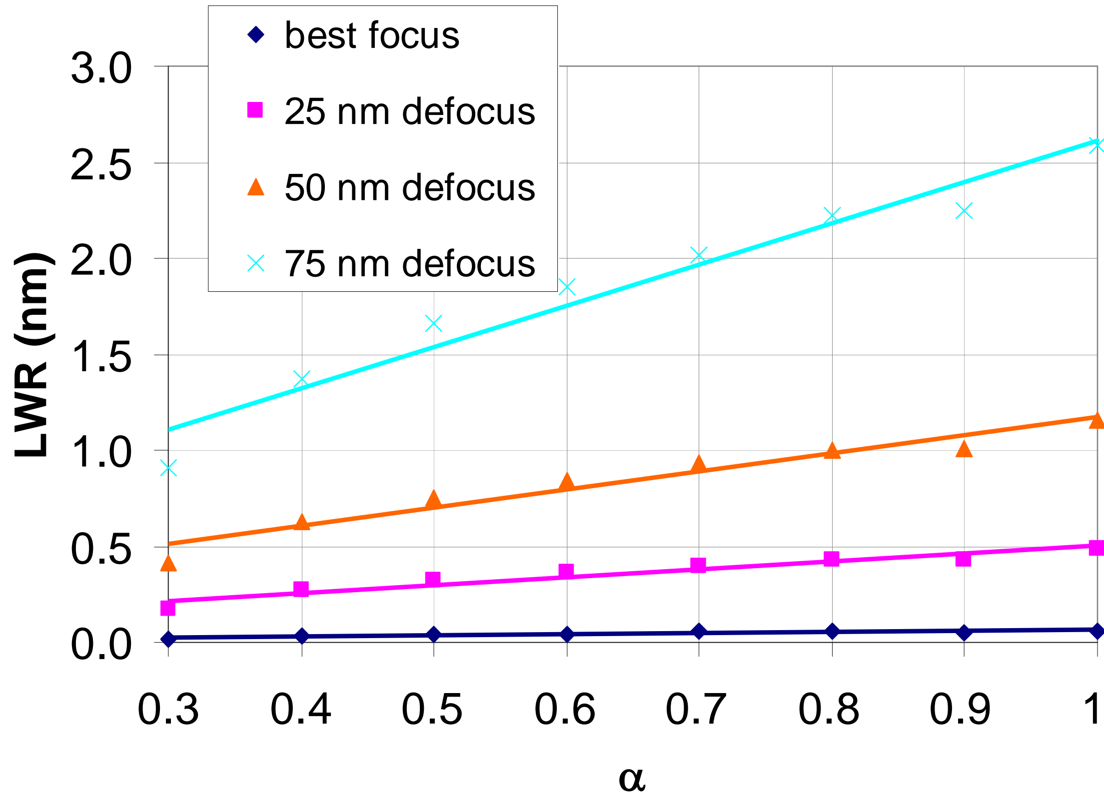

Fig. 4. LWR as a function of roughness exponent (α) assuming 0.32 NA, 22-nm half-pitch lines, disk illumination with a Sigma of 0.5, flare of 5%, RSR of 100 pm, and correlation length of 100 nm. Response is linear with the roughness exponent which serves to modulate the amount of roughness in the passband of interest. Thus the roughness exponent has a similar effect as directly changing the RSR.

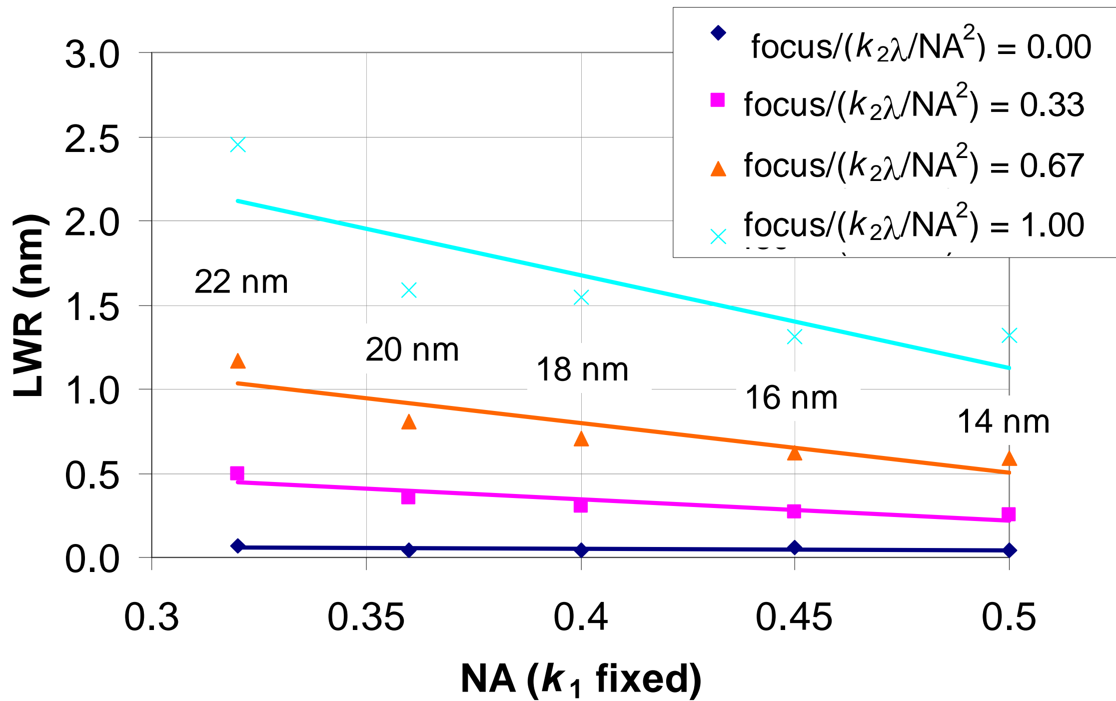

Fig. 5. Effect of changing the NA with fixed k_1. Defocus range is scaled by NA^2, thus plot can be viewed as a function of half-pitch technology node shown as labels in the pole. In all cases the Sigma is kept at 0.5, flare kept at 5%, roughness correlation length kept at 100 nm, RSR kept at 100 pm, and roughness exponent kept at 1.

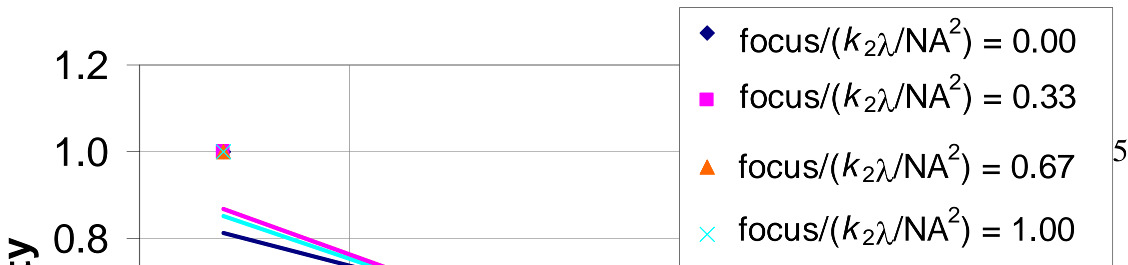

Fig. 6. Difficulty ($LWR/LWR_{0.32NA}/CD$) as a function of NA. A value of 1 represents the difficultly at 0.32 NA. Decreasing values represents less difficulty. Difficulty is inversely proportional to the required RSR to meet the LWR requirements.

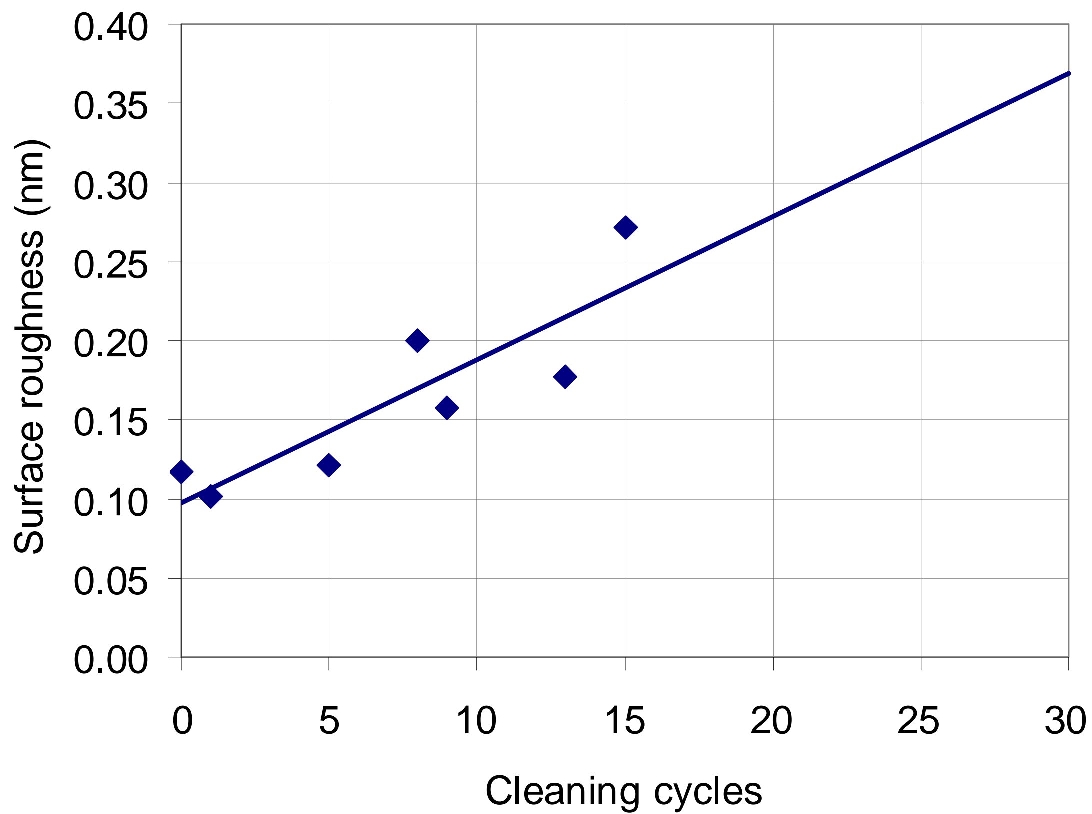

Fig. 7. Measured ruthenium capping layer roughness as a function of cleaning cycles. Also shown is a linear fit to the data extrapolating the damage out to 30 cleaning cycles.

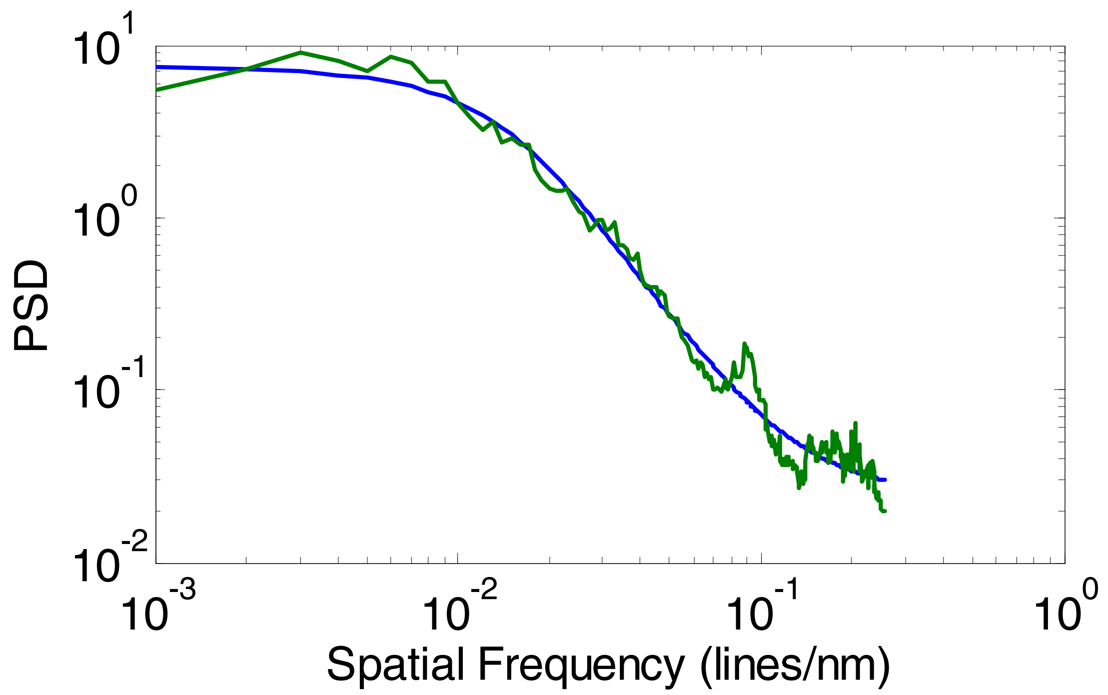

Fig. 8. Measured power spectrum for roughness data in Fig. 7.

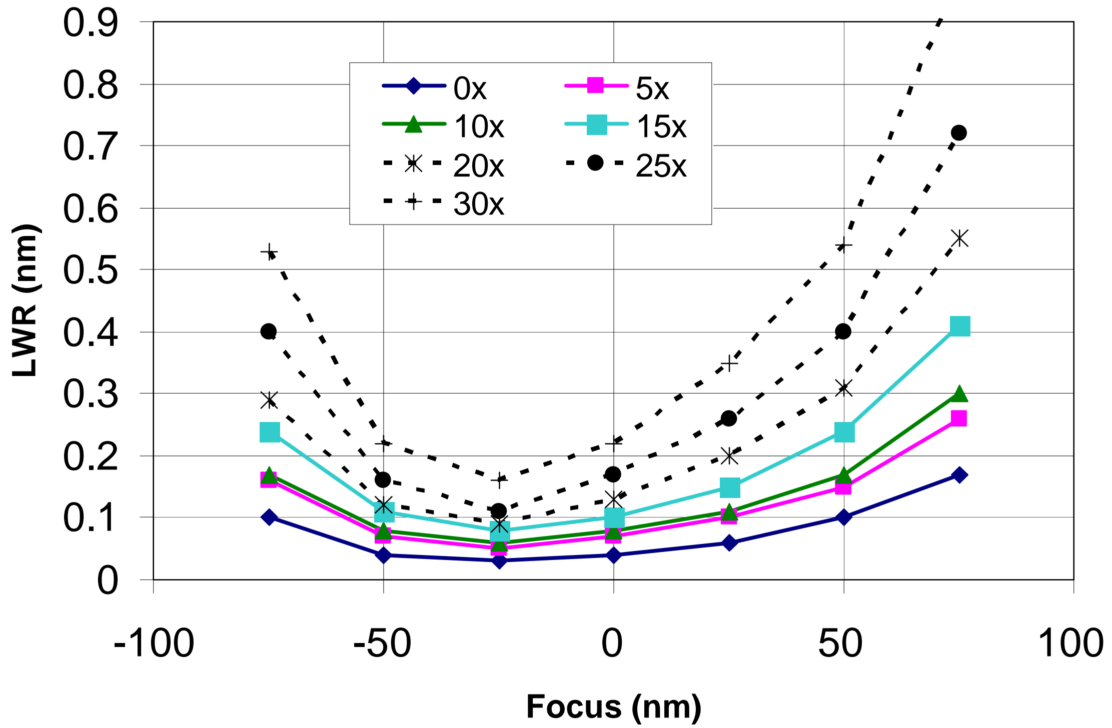

Fig. 9. Computed LWR for the measured and extrapolated ruthenium capping layer roughness. The results show near 1 nm LWR at the edge of focus after 30 cleaning cycles. The asymmetric through focus behavior is a result of combined phase and amplitude roughness in the reflected field.

DISCLAIMER

This document was prepared as an account of work sponsored by the United States Government. While this document is believed to contain correct information, neither the United States Government nor any agency thereof, nor The Regents of the University of California, nor any of their employees, makes any warranty, express or implied, or assumes any legal responsibility for the accuracy, completeness, or usefulness of any information, apparatus, product, or process disclosed, or represents that its use would not infringe privately owned rights. Reference herein to any specific commercial product, process, or service by its trade name, trademark, manufacturer, or otherwise, does not necessarily constitute or imply its endorsement, recommendation, or favoring by the United States Government or any agency thereof, or The Regents of the University of California. The views and opinions of authors expressed herein do not necessarily state or reflect those of the United States Government or any agency thereof or The Regents of the University of California.